Journal for ImmunoTherapy of Cancer

RIG-I agonists promote antigen-spreading and facilitate durable CAR-T responses in pancreatic ductal adenocarcinoma

Anne Marie Senz,[1] Bruno L Cadilha,[2] Julia Teppert,[1] Simone Formisano,[1] Charlotte Marx,[1] Theo Lorenzini,[1] Daniel F R Boehmer,[1,3] Christine Hoerth,[1] Simon Delahais,[1] Stefan Endres ,[1,4,5] Peter Duewell ,[6] Max Schnurr,[1] Sebastian Kobold ,[1,4,5,7] Lars M Koenig [1]

To cite: Senz AM, Cadilha BL, Teppert J, *et al*. RIG-I agonists promote antigen-spreading and facilitate durable CAR-T responses in pancreatic ductal adenocarcinoma. *Journal for ImmunoTherapy of Cancer* 2026;**14**:e013282. doi:10.1136/jitc-2025-013282

► Additional supplemental material is published online only. To view, please visit the journal online (https://doi.org/10.1136/jitc-2025-013282).

AMS and BLC contributed equally.

Accepted 29 December 2025

For numbered affiliations see end of article.

Correspondence to
Dr Lars M Koenig;
lars.koenig@med.uni-muenchen.de

ABSTRACT

Background Pancreatic ductal adenocarcinoma (PDAC) remains largely refractory to chimeric antigen receptor (CAR)-T cell therapy. Insufficient T cell infiltration, a highly immunosuppressive microenvironment, and antigen loss pose major challenges for CAR-T cell therapy.

Methods We investigated therapeutic synergies of synthetic 5′-triphosphate RNA (3p-RNA), an agonist of the cytoplasmic double-stranded RNA sensor Retinoic Acid Inducible Gene I (RIG-I), and CAR-T cell therapy using syngeneic and human xenograft PDAC models. Tumor growth, chemokine secretion, immune-cell composition, CAR-T persistence, and endogenous T cell responses were assessed by flow cytometry, multiplex cytokine arrays, Enzyme-linked Immunospot (ELISpot), and vaccination-challenge.

Results 3p-RNA provoked rapid type I interferon accompanied with chemokine ligand CCL5 and CXCL9/10/11 secretion, creating chemokine gradients that recruited chemokine receptor $CCR5^+$/$CXCR3^+$ CAR-T cells into tumors. RIG-I activation enhanced CAR-T cell proliferation, activity, and CAR-T persistence. Combination therapy eradicated established tumors in 60%–70% of mice, whereas either monotherapy was largely ineffective. Cured animals rejected CAR antigen-negative tumor cell rechallenge, demonstrating antigen-spreading and endogenous T cell responses.

Conclusions Intratumoral RIG-I priming reprograms the PDAC microenvironment, transforming a non-responsive cancer into a CAR-T-permissive one, supporting durable, poly-antigenic immunity. These findings position 3p-RNA as a rapid, clinically tractable co-therapy to extend CAR-T efficacy to solid tumors.

WHAT IS ALREADY KNOWN ON THIS TOPIC

⇒ CAR-T cell therapy has shown limited efficacy in solid tumors, such as pancreatic ductal adenocarcinoma (PDAC), due to immune exclusion, stromal barriers, and antigen escape. Synthetic RIG-I agonists like 3p-RNA can trigger innate immune activation but have not yet translated into durable responses as monotherapy.

WHAT THIS STUDY ADDS

⇒ This study demonstrates that local priming with 3p-RNA enhances CAR-T cell infiltration, survival, and function in PDAC, leading to sustained tumor regression. Interestingly, the combination facilitated antigen-spreading leading to CAR target-independent endogenous T cell response.

HOW THIS STUDY MIGHT AFFECT RESEARCH, PRACTICE OR POLICY

⇒ The findings support clinical translation of RIG-I agonist priming as a co-therapy with CAR-T cells in solid tumors. This approach may broaden the applicability of CAR-T cell therapy beyond hematological malignancies, especially in immune-excluded cancers like PDAC.

BACKGROUND

Pancreatic ductal adenocarcinoma (PDAC) is projected to become the second leading cause of cancer-related mortality by 2030, and its 5-year survival rate remains below 12% despite incremental improvements from folinic acid, fluorouracil, irinotecan, and oxaliplatin and gemcitabine/paclitaxel chemotherapy.[1] Immunotherapies that have transformed therapy of hematological malignancies have delivered only limited efficacy in PDAC.[2 3] Immune checkpoint blockade and early chimeric antigen receptor (CAR)-T trials have so far yielded only transient benefits in PDAC with pembrolizumab producing an objective response rate of only ≤3% with a median overall survival of ~4 months in the KEYNOTE-158 cohort. Mesothelin-specific and Prostate-Specific Membrane Antigen-directed CAR-T cells were safe but achieved only short-lived tumor shrinkage. CLDN18.2-directed CAR-T cells recently have shown improved outcomes,[4 5] but results still fall

short in comparison to non-solid tumors, underscoring the need for rational combination strategies.[2 6 7]

PDAC is characterized by a highly immunosuppressive microenvironment composed of a dense extracellular matrix, tumor-associated macrophages (TAMs), myeloid-derived suppressor cells (MDSCs), and regulatory T cells that sculpt an immunosuppressive cytokine milieu, among others dominated by TGF-β, IL-10, and arginase-1, that blunts T cell activation. Its pronounced genomic and antigenic heterogeneity enables rapid outgrowth of tumor clones that downregulate the targeted antigen, leading to immune escape and limiting durable control.[8–13] Resistance persists even when CAR-T cells manage to infiltrate the tumor, underlining the need for complementary interventions that both sensitize tumor cells and initiate lasting immunity. Reflecting these headwinds, recent Society for Immunotherapy of Cancer guidelines emphasize that future PDAC immunotherapy will require multimodal combinations that modulate both stroma and intrinsic tumor properties.[14] One approach to overcoming tumor antigen loss is provoking an immune response that triggers antigen spreading, a process whereby initial tumor lysis releases additional neoantigens that are cross-presented to naïve T cells. This endogenous immune activation is hypothesized to generate immune memory, a state in which the immune system is capable of recognizing and targeting residual or recurrent tumor cells in the long term, thus reducing the likelihood of relapse. This broadening of the endogenous T cell receptor (TCR) repertoire has been shown in melanoma and glioma models and was closely associated with sustained tumor control and resistance to escape variants.[15 16] While endogenous T and NK cell cytotoxicity induces immunogenic cell death (ICD), which promotes the initiation of de novo immune responses,[17 18] the immunogenic potential of CAR-T-mediated cytotoxicity remains highly debated.

Recent evidence suggests that restoring RIG-I/MAVS signaling can resensitize tumors to cytotoxic lymphocytes.[19] Activation of innate RNA sensing pathways offers a means to remodel the tumor microenvironment (TME) without overt systemic toxicity. A compelling example of this strategy involves short double-stranded 5'-triphosphate RNA (3p-RNA), which is a potent agonist of the retinoic acid-inducible gene I (RIG-I) receptor.[20] On binding to 3p-RNA, RIG-I undergoes a conformational change that activates MAVS-dependent IRF3/NF-κB downstream signaling pathways, leading to the production of type I interferons (IFNs) and the secretion of proinflammatory cytokines and chemokines. We have shown earlier that RIG-I-like receptor (RLR) activation by 3p-RNA provokes an immunogenic form of tumor-cell death marked by calreticulin exposure, HMGB1 release, and type I interferon, which licenses $CD8\alpha^+$ dendritic cells (DCs) to cross-present tumor antigen and activate naïve $CD8^+$ T cells. The same stimulus upregulates MHC-I and Fas on surviving tumor cells, rendering them exquisitely sensitive to cytotoxic T lymphocyte attack.[21] Additionally, RLR activation was shown to induce functional reprogramming of the myeloid compartment into an anti-tumor-directed M1-like state and an increased $CD8^+$ T cell infiltration into TME; however, this is insufficient for complete tumor regression.[10] Based on these findings, we hypothesized that combining innate immune signaling with CAR-T cell therapy enhances the therapeutic response against solid tumors. Here, we test whether 3p-RNA can precondition the PDAC microenvironment to (1) increase immune cell infiltration and activity, (2) sensitize tumor cells toward CAR-T cell-mediated killing, and (3) ignite a broad intrinsic antitumor response for relapse protection.

METHODS

Cell line generation and culture

The murine KPC-derived T110299 tumor cell line (kindly provided by Prof. Jens Siveke, University Hospital Essen, Germany, and previously described by Metzger *et al*[11 12], was retrovirally engineered to express the murine EpCAM protein (UNIPROT entry Q99JW5). The resulting T110299-EpCAM cell line was transfected with linearized pAC-Neo-OVA plasmid and selected with 1 mg/mL G418 (Invivogen) to generate T110299-EpCAM-OVA tumor cells. The human SUIT-2-MSLN tumor cell line has been previously described.[22] Surface expression of EpCAM or human mesothelin (MSLN) in the tumor cell lines was verified by flow cytometry using anti-mouse CD326 (118210, Biolegend) or anti-human mesothelin (FAB32652, RnD Systems), respectively. OVA expression was confirmed in cytotoxicity assays using OT-I T cells. All cell lines were cultured as previously described[19] unless otherwise noted. Retroviral vectors (pMP71) encoding CAR or chemokine receptors were introduced into packaging cell lines for virus production as previously described.[23] All cell lines used in experiments were routinely tested for mycoplasma contamination using the MycoAlert Detection Kit (LT07-318, Lonza).

3p-RNA generation and tumor cell transfection

Double-stranded 3p-RNA was synthesized from a DNA template using the HiScribe T7 Quick High Yield RNA Synthesis Kit (E2050L, New England Biolabs), followed by DNase I digestion for 15 minutes at 37°C. RNA was then purified using the RNA Cleanup and Concentration Kit (43200, Norgen Biotek). For in vitro transfection, tumor cells were seeded at 1.2×10^4 cells per well in 96-well flat-bottom plates or 2×10^5 cells per well in 6-well plates. RNA was transfected using Lipofectamine RNAiMAX (13778150, Invitrogen). T110299-EpCAM and T110299-EpCAM-OVA cells were transfected with 160 nM RNA, complexed with 0.9 µL RNAiMAX per well in 96-well plates, in tumor cell medium supplemented with 2% FCS (Gibco). SUIT-02-MSLN cells were transfected with 80 - 160 nM RNA, complexed with 0.15–0.3 µL RNAiMAX per well, and cultured in tumor media with 10% FCS.

T cell transduction and culture

Second-generation CAR constructs included a single-chain variable fragment derived from murine anti-EpCAM (clone G8.8) or human anti-mesothelin (clone SS1) antibodies, linked to CD28 and CD3ζ intracellular signaling domains. Chemokine receptor constructs were generated by overlap extension PCR and recombinant cloning of full-length receptors linked to GFP via a 2A sequence.[23] Retroviral transduction of murine splenocytes was performed following activation with 1 µg/mL murine anti-CD3 (16-0031-82, Invitrogen) and 0.1 µg/mL murine anti-CD28 (16-0281-82, Invitrogen) antibodies, with expansion in murine T cell media supplemented with IL-15 (200-15, Peprotech) every second day as previously described.[22] Human CAR-T cells were generated by retroviral transduction of activated PBMCs from healthy donors as previously described.[24] Transduction efficiency was verified by flow cytometry.

Migration assay

Migration of chemokine receptor-transduced T cells toward the supernatant of 3p-RNA-transfected or control-transfected T110299-EpCAM cells was assessed in 3 µm pore transwell plates (3386, Corning) as described.[25] Transduced T cells (5×10^5) were seeded in the upper chamber, and cells migrating to the lower chamber after 4 hours at 37°C were analyzed by flow cytometry.

T cell proliferation and cytotoxic assays

T cell proliferation was assessed using 5-ethynyl-2′-deoxyuridine (EdU) incorporation. T cells were cultured for 24 hours in the presence of 10 µM Click-iT EdU (C10418, Invitrogen), stained and fixed according to the manufacturer's instructions, and analyzed by flow cytometry.

Cytotoxicity was measured using either the xCELLigence Real-Time Cell Analysis system (Agilent) or the Incucyte Live-Cell Analysis System (Sartorius). The xCELLigence platform quantifies tumor cell adhesion as a proxy for viability, whereas the Incucyte system monitors changes in cell confluence and uptake of Incucyte Cytotox Green dye (Sartorius, #4633), which was added at 250 nM to assess tumor-cell death. For xCELLigence assays, tumor cells (2×10^4 per well) were transfected with 3p-RNA or control RNA and seeded in 96-well E-plates. Once the cell index reached 1, CAR-T cells were added at the effector-to-target (E:T) ratios specified in the figure legends. Cell index values were normalized to the time point of effector cell addition. For Incucyte assays, tumor cells (1×10^4 per well) were seeded in 96-well flat-bottom plates and transfected 6 hours after plating with 3p-RNA or left untreated. 24 hours after tumor-cell seeding, CAR-T cells were added at a 1:1 E:T ratio.

Quantitative RT-PCR of chemokine expression and cytokine secretion quantification

Tumor cells were harvested 6 hours post-transfection for RNA isolation using the RNeasy Plus Mini Kit (74134, Qiagen). cDNA was synthesized using the RevertAid First Strand cDNA Synthesis Kit (K1622, Thermo Scientific). qPCR primers were designed using Roche's Universal ProbeLibrary based on NCBI GenBank sequences. Amplification was performed on the Roche LightCycler 480 II. Supernatant cytokine levels were quantified by ELISA for murine IFN-γ, Granzyme B, and IFN-β (DY485, DY1865, and DY8234-05, respectively; R&D Systems). ELISpot was used to quantify IFN-γ spot-forming units in splenocytes (2×10^5 cells per well) stimulated for 24 hours with SIINFEKL peptide using the Mouse IFN-γ T Cell ELISpot Kit (CT317-PR5, U-CyTech).

Tumor growth studies and treatments

All animal experiments were approved by the local regulatory agencies (Regierung von Oberbayern). Female C57BL/6J mice (Charles River) were subcutaneously implanted with 10^6 T110299-EpCAM cells (with or without OVA). When average tumor size reached ~9 mm², mice were randomized and treated intratumorally with 10 µg 3p-RNA complexed with in vivo-jetPEI (VWR International, Darmstadt, Germany) with an amine to phosphate (N/P) ratio of 6 or phosphate buffered saline (PBS). Six hours later, 10^7 transduced T cells (>30% anti-EpCAM CAR$^+$) were injected intravenously. Intratumoral injections of 3p-RNA were repeated as indicated. Tumor size was measured every two days by a blinded observer. To assess CAR-T cell infiltration and TME composition, mice were euthanized at day 3 post-treatment in specific experiments. OVA-specific T cells were evaluated at day 9. Human CAR-T cell infiltration was assessed in NXG mice (Janvier) inoculated with 10^6 SUIT-2-MSLN cells under the same treatment protocol.

Mouse vaccination with in vitro killed tumor cells

T110299-EpCAM-OVA cells (1.2×10^6) were co-cultured for 48 hours with anti-EpCAM CAR-T cells, with or without prior transfection of 160 nM 3p-RNA or treated with 5 µM staurosporine. Cell debris and supernatant were collected and used to vaccinate C57BL/6J mice subcutaneously in the right flank. After 6 days, mice were challenged with 0.5×10^6 T110299 cells in the opposite flank. Tumor volume was measured every 2 days.

Organ and single-cell preparation

Spleens were mashed through 70 µm strainers, and red blood cells were lysed with ammonium chloride-Tris (ACT) buffer. Erythrocyte lysis in blood, collected via heparinized capillary tubes, was performed using BD Pharm Lyse (555899, BD Biosciences). Tumors were dissected into 1–2 mm² pieces and enzymatically digested using the Tumor Dissociation Kit (130-096-730, Miltenyi Biotec) and gentleMACS Dissociator.

Flow cytometry

Single-cell suspensions were stained in PBS with 2% FCS and 2 mM EDTA. Dead cells were excluded using fixable viability violet dye (65-0865-18, Invitrogen). Surface markers were stained for 30 min at 4°C; chemokine

receptors were stained at 37°C for 15 min. Absolute cell counts were obtained using CountBright counting beads (C36950, Invitrogen). Acquisition was performed using BD FACSCanto II or BD LSRFortessa cytometers and analyzed using FlowJo V.10.3.

Statistical analysis

Data are presented as mean±SD or SEM, as indicated in figure legends. For mouse experiments, group means with SEM were used. Statistical comparisons between groups were made using one-way or two-way analysis of variance, with Dunnett's or Bonferroni's post-tests, one-sample or two-sample t-tests, or Mann-Whitney U test as described in figure legends. Significance thresholds were defined as p<0.05, with specific thresholds indicated (* for p<0.05, ** for p<0.01, *** for p<0.001, and **** for p<0.0001). Analyses were performed using GraphPad Prism (V.8, GraphPad Software), with replicates (n) specified in the figure legends.

RESULTS

Engineering and validation of a preclinical PDAC tumor model for combined CAR-T cell and RIG-I-targeted therapy

To evaluate whether RIG-I activation in the TME can enhance the efficacy of CAR-T cells in solid tumors such as PDAC, we used a tumor model that recapitulates key features observed in human disease where limited immunotherapeutic benefit was observed. We selected the T110299 tumor cell line, which is derived from tumors of *LSL-Kras$^{G12D/+}$;LSL-Trp53$^{R172H/+}$;Pdx-1-Cre (KPC)* mice. Isolated cell lines from these tumors retain desmoplastic TME with low T cell and high macrophage infiltration.[11] We used an established murine CAR construct targeting murine epithelial cell adhesion molecule (in short, EpCAM) that has preclinically validated data in murine tumor models.[23 26] T110299-EpCAM was generated by means of a stable retroviral transduction and polyclonal sorting process. EpCAM-specific CAR-T cells were able to recognize T110299-EpCAM cells in a dose-dependent manner (figure 1a, online supplemental Figure 1a) but not T110299 cells (figure 1b, online supplemental Figure 1b). T110299-EpCAM preserved functional RIG-I and IFN sensing pathways as shown by IFN-β secretion upon 3p-RNA stimulation (figure 1c). Furthermore, 3p-RNA-stimulated T110299-EpCAM cells upregulated MHC-I (figure 1d) underpinning the potential for 3p-RNA therapy to synergize with adoptive T cell therapy in solid tumors by enhancing antigen presentation and triggering an inflammatory signature in the TME.[27] As observed in previous work,[28] tumor cell transfection with 3p-RNA does not induce significant killing effects in T110299-EpCAM cells in vitro (figure 1e, online supplemental Figure 1c).

3p-RNA and CAR-T cells synergize for improved anti-tumoral efficacy in murine and human pancreatic tumor models

3p-RNA and CAR-T cells have distinct killing mechanisms[21 29 30] that may synergize in the killing of tumor cells in a combination setting. To test this hypothesis, we performed co-cultures of anti-EpCAM CAR-T cells and T110299-EpCAM tumor cells with and without 3p-RNA. Samples treated with the combination of 3p-RNA and CAR-T cells demonstrated faster cell-killing kinetics than the monotherapy (figure 2a–c, as well as online supplemental Figure 1d and e and online supplemental Figure 2a). To understand the mechanism behind the enhanced cytotoxicity, we analyzed CAR-T cell activation and effector function 24 hours post co-culture. CAR-T cells exposed to 3p-RNA-transfected tumor cells exhibited higher CD69 surface expression (figure 2d) and increased degranulation of IFN-γ and Granzyme B (figure 2e,f, as well as online supplemental Figure 1f and g). These findings were confirmed in a human in vitro

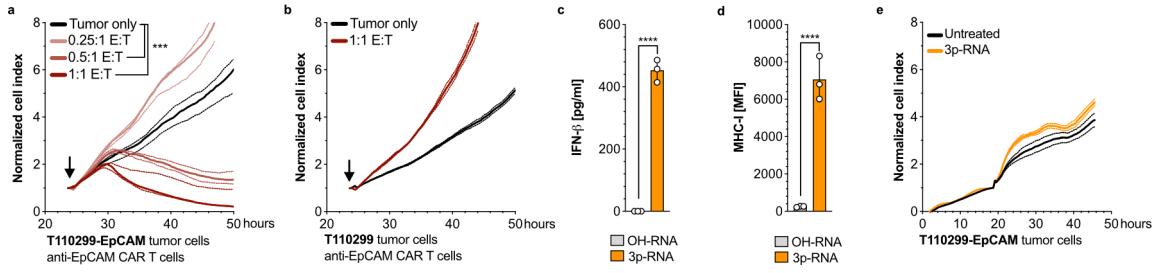

Figure 1 The novel T110299-EpCAM murine pancreatic tumor model can be targeted by murine anti-EpCAM CAR-T cells and is sensitive to 3p-RNA stimulation in vitro. (a, b) Real-time impedance-based cytotoxicity assays (xCELLigence) tracking the growth of T110299-EpCAM (a) and T110299 (b) tumor cells as a proxy for CAR-T cell-mediated lysis when co-cultured with anti-EpCAM CAR-T cells at three effector-to-target (E:T) ratios: 0.25:1, 0.5:1, and 1:1. Arrows denote the time at which CAR-T cells were added to the culture. (c) ELISA measurement of murine IFN-β in the supernatant of T110299-EpCAM tumor cells 24 hours post-transfection with either 3p-RNA or OH-RNA control. (d) Analysis of MHC-I surface expression by flow cytometry on T110299-EpCAM cells 24 hours after transfection with 3p-RNA or OH-RNA at a concentration of 160 nM. (e) Real-time impedance-based cytotoxicity assays tracking the growth of T110299-EpCAM tumor cells when treated with 160 nM 3p-RNA. Data shown are representative of three independent experiments (a–e) with error bars representing mean values±SD of technical replicates from the experiment shown. Statistical significance was determined by two-tailed t-tests for (c, d) and two-way ANOVA for (a, b, e).*** p<0.001, **** p<0.0001. If no statistics are shown, a significance of p<0.05 was not achieved. ANOVA, analysis of variance; MHC-I, major histocompatibility complex I; MFI, mean fluorescence intensity.

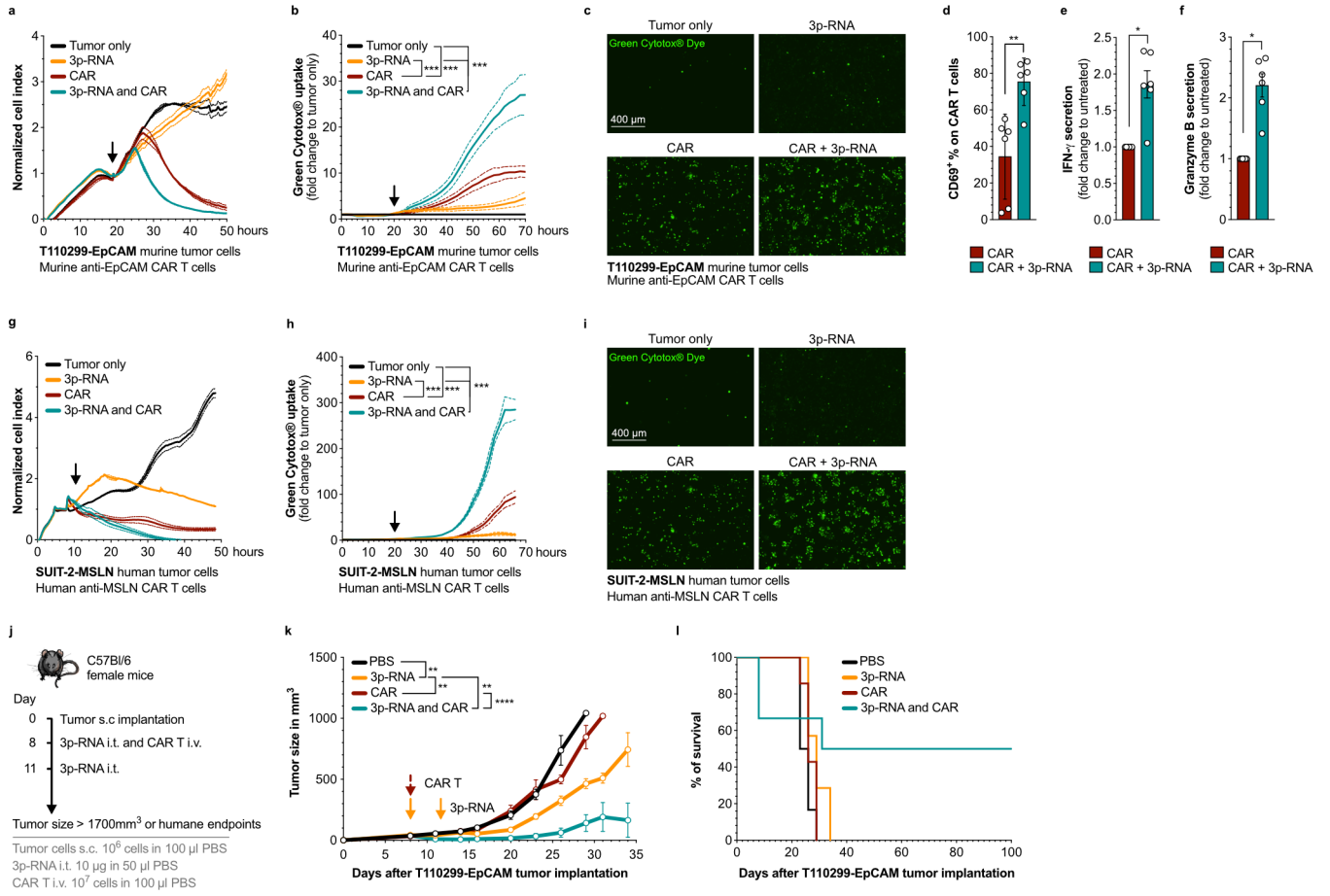

Figure 2 3p-RNA and CAR-T cells synergize for more potent antitumor efficacy. (a) Real-time cytotoxicity of murine T110299-EpCAM tumor cells measured by xCELLigence at a 10:1 effector-to-target (E:T) ratio, and (b, c) Incucyte Cytotox Green-based quantification of tumor-cell lysis at a 1:1 E:T ratio, with or without 3p-RNA treatment (160 nM). Arrow depicts the time point of CAR-T cell addition. Data are representative of 2–3 independent experiments. Differences between groups were analyzed using two-way ANOVA with Tukey's correction for multiple comparisons. (d, e, f) CD69 expression (d) and secretion of IFN-γ (e) and Granzyme B (f) by anti-EpCAM CAR-T cells after 24-hour co-culture with T110299-EpCAM tumor cells transfected with 3p-RNA or controls. Data represent mean±SD of 3–6 independent experiments. Statistical analysis for (d) was performed using a Mann-Whitney U test. Statistical analysis for (e, f) was performed using a Wilcoxon signed rank test. (g) Real-time cytotoxicity of murine Suit-2-MSLN tumor cells measured by xCELLigence at a 2.5:1 E:T ratio, and (h, i) Incucyte Cytotox Green-based quantification of tumor-cell lysis at a 1:1 E:T ratio, with or without 3p-RNA treatment (80 nM). Arrow depicts the time point of CAR-T cell addition. Data are representative of 2–3 independent experiments. Differences between groups were analyzed using two-way ANOVA with Tukey's correction for multiple comparisons. (j) Schematic representation of the in vivo tumor challenge experimental timeline. (k) Tumor growth curve of T110299-EpCAM in mice treated with 10 µg 3p-RNA complexed to in vivo-JetPEI and/or 10^7 total T cells, of which at least 30% were anti-EpCAM CAR-T cells (n≥5 mice per group). (l) Survival plots of the treatment experiment are depicted in (k). In vivo error bars represent mean±SEM. Differences between groups were analyzed using two-way ANOVA with Bonferroni correction for multiple comparisons. *p<0.05, **p<0.01, *** p<0.001, ****p<0.0001. ANOVA, analysis of variance; PBS, phosphate buffered saline.

system using a mesothelin-transduced pancreatic tumor cell line, SUIT-2 (SUIT-2-MSLN),[26] and human anti-Mesothelin CAR-T cells (figure 2g–i, as well as online supplemental Figure 1h and i and online supplemental Figure 2b). To evaluate the effect in vivo, we treated mice bearing subcutaneous T110299-EpCAM tumors with either monotherapy or combination therapy (figure 2j). While CAR-T cells alone had minimal effect and 3p-RNA alone induced only transient tumor growth delay, the combination treatment led to complete tumor rejection in 3 of 6 mice (figure 2k,l). Notably, although it was confirmed that the C57BL/6 T110299 model exhibits some type I IFN responsiveness, 3p-RNA alone does not induce durable tumor eradication (Figure k). Instead, we postulate that the 3p-RNA creates a CAR-T-permissive therapeutic window in this model, which we intend to further mechanistically characterize.

RIG-I activation remodels the TME, enhances CAR-T cell infiltration and proliferation

PDAC is characterized by an immunosuppressive milieu in which an increased infiltration of MDSCs and TAMs coincides with an exclusion of T cells.[11] We have shown earlier that the myeloid compartment in the TME can

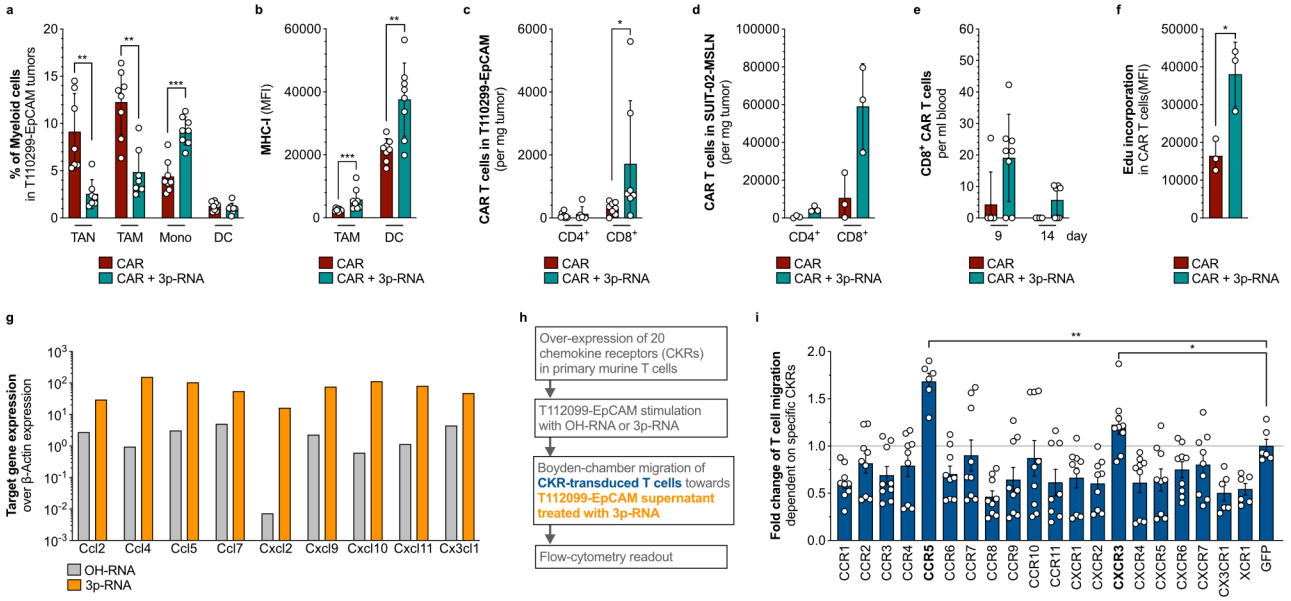

Figure 3 3p-RNA remodels the PDAC microenvironment, enhances CAR-T cell persistence, proliferation, and chemokine-driven infiltration. (a) C57BL/6 mice bearing T112099-EpCAM tumors were treated with 10^7 adoptively transferred T cells (at least 30% were anti-EpCAM CAR$^+$) with or without 10 µg 3p-RNA complexed to in vivo-JetPEI. Tumors were explanted 3 days post-treatment for flow cytometry analysis. Frequency of live CD11b$^+$ Ly6C^{int} Ly6G$^+$ (tumor-associated neutrophils, in short TAN), CD11b$^+$ Ly6C$^-$ F4/80$^+$ (tumor-associated macrophages, in short TAM), CD11b$^+$ Ly6C^{high} Ly6G$^-$ (Monocytes, in short Mono), and CD11b$^+$ CD11c$^+$ MHC-II$^+$ (dendritic cells, in short DC) in tumors. (b) MHC-I expression on TAM and DC. (c, d) CD4$^+$ or CD8$^+$ CAR-T cell counts in pancreatic murine tumors (c) and in pancreatic human xenograft tumors (d). (e) Counts of CD8$^+$ CAR-T cells in blood on days 9 and 14 after adoptive cell transfer in T112099-EpCAM tumor-bearing mice. (f) Proliferation of CD8$^+$ CAR-T cells, assessed via EdU incorporation, when co-cultured with untreated or 3p-RNA-transfected T110299-EpCAM tumor cells in vitro. (g) Quantitative real-time PCR (qPCR) of chemokine expression in T110299-EpCAM tumor cells 24 hours post-transfection with 3p-RNA or OH-RNA control. Only chemokines with significant induction are depicted. (h) Schematic of individual chemokine receptor functional probing in primary murine T cells. Migration toward supernatants from T110299-EpCAM tumor cells transfected with 3p-RNA or OH-RNA was assessed using a Boyden chamber. (i) Flow-cytometry readout of specific migration of CKR-transduced T cells toward supernatant of 3p-RNA-stimulated cells. For each biological replication, a fold change of migration toward supernatants from OH-RNA (control) and 3p-RNA-stimulated cells was calculated, and each CKR-transduced T cell was then normalized to GFP-transduced control T cells. The dashed gray line depicts the baseline for said GFP-control transduced T cells. Error bars indicate mean±SEM (n=8 mice, for (a–c, e); n=3 mice, for (d)) for in vivo data and mean±SEM (n=2 technical duplicates, for (g); n=6–9 technical replicates pooled from three independent experiments for (i)) for in vitro data. Statistical analysis for TME composition, MHC expression, CAR-T cell infiltration, and T cell migration was performed using Mann-Whitney U test. In vitro proliferation was analyzed using unpaired two-sample t-tests. *p<0.05, **p<0.01, ***p<0.001. PDAC, pancreatic ductal adenocarcinoma. MHC-I, major histocompatibility complex I; CKRs, chemokine receptors.

be functionally reprogrammed from suppressive to pro-inflammatory phenotype using RIG-I-like helicase agonists.[11] To understand if this holds true in the CAR-T cell combination setting, we performed flow cytometric analysis of tumors treated with CAR-T cells alone or in combination with 3p-RNA. Tumors from mice receiving the combination therapy showed a significant decrease in the relative frequency of tumor-associated neutrophils (TAN), often referred to as polymorphonuclear (PMN)-MDSC, and TAM, within the CD11b$^+$ immune cell fraction, accompanied by a marked increase of Ly6C$^+$ inflammatory monocytes (figure 3a). Furthermore, it was evident that although the relative frequency of DC remained unchanged (figure 3a), the surface expression of MHC-I was significantly upregulated in the presence of 3p-RNA in both DC and TAM populations (figure 3b). These changes in the myeloid compartment coincide with an increase in intratumoral CD8$^+$ CAR-T cells, observed in both the murine T110299-EpCAM tumor model (figure 3c) and the human SUIT-2-MSLN xenograft model (figure 3d).

Limited proliferation and poor persistence of CAR-T cells are major barriers to effective treatment of both hematological malignancies and solid tumors, where the TME further restricts T cell expansion and survival.[31] To evaluate whether 3p-RNA treatment could enhance CAR-T cell persistence, we used flow cytometry to quantify circulating CAR-T cells in peripheral blood at multiple time points. Notably, these experiments were performed without lymphodepleting preconditioning—a regimen typically used to enhance CAR-T cell engraftment and expansion by reducing competition from endogenous lymphocytes and increasing the availability of homeostatic cytokines. Mice receiving the combination treatment consistently exhibited higher numbers of circulating CAR-T cells, whereas mice treated with CAR-T cell monotherapy had no detectable CAR-T cells in circulation by day 14 (figure 3e). In vitro, we observed that

CAR-T cells cultured with tumor cells that were treated with 3p-RNA had a higher proliferation rate measured by 5-ethynyl-2'-deoxyuridine (EdU)-incorporation (figure 3f). These findings suggest that 3p-RNA positively influences CAR-T cell proliferation and persistence.

Chemokine ligands and their cognate chemokine receptors are known orchestrators of immune responses with the potential to steer infiltration of immune cell subtypes and even drive critical signaling crucial for immune cell proliferation.[32] RIG-I activation induces a plethora of chemokines that could facilitate CAR-T cell infiltration into the TME. To get a better understanding of the relevant chemotactic cues, we established a chemokine expression profile of T110299-EpCAM tumor cells transfected with 3p-RNA or OH-RNA control indicated by qPCR analysis. A variety of chemokines were highly induced, among which several could attract T cells (figure 3g). To evaluate the relevance of upregulated chemokines in mediating CAR-T cell migration, we used a gain-of-function approach and transduced primary murine T cells to express each chemokine receptor individually and probed them on a Boyden chamber migration assay for migration toward 3p-RNA-treated tumor cell supernatant (figure 3h). A significant fold increase of the migration of CCR5- and CXCR3-transduced T cells toward 3p-RNA-treated tumor cell supernatant was observed (figure 3i) aligning well to the observed increase in their cognate chemokines CCL4, CCL5, and CXCL9, 10, 11, respectively. Together, these data suggest that RIG-I activation of T110299-EpCAM TME can induce the expression of a variety of chemokines, with physiologically relevant attraction of CAR-T cells through a CCR5 and CXCR3-dependent mechanism.

3p-RNA-triggered ICD potentiates CAR-T therapy antigen spreading and induces de novo responses in PDAC models

Antigen loss is the most frequent cause of relapse in patients who initially respond to CAR-T cell therapy.[13] Cell death induction mediated by 3p-RNA has been previously described to induce an immunogenic form of cell death,[21] which can consequently drive antigen spreading and potentially assist with the mounting of endogenous anti-tumoral T cell clonal expansions for long-lasting tumor control. Cell surface exposure of calreticulin is a known hallmark of ICD.[33] In both murine (figure 4a) and human (figure 4b) in vitro PDAC models, CAR-T cell-mediated killing did not induce calreticulin exposure. In contrast, adding 3p-RNA as a combination partner potentiated ICD, as evidenced by increased calreticulin expression. To assess whether this enhanced ICD translated into improved endogenous immune responses, we employed a model neoantigen system using OVA. Mice bearing subcutaneous T110299-EpCAM-OVA tumors were treated with 3p-RNA and anti-EpCAM CAR-T cells

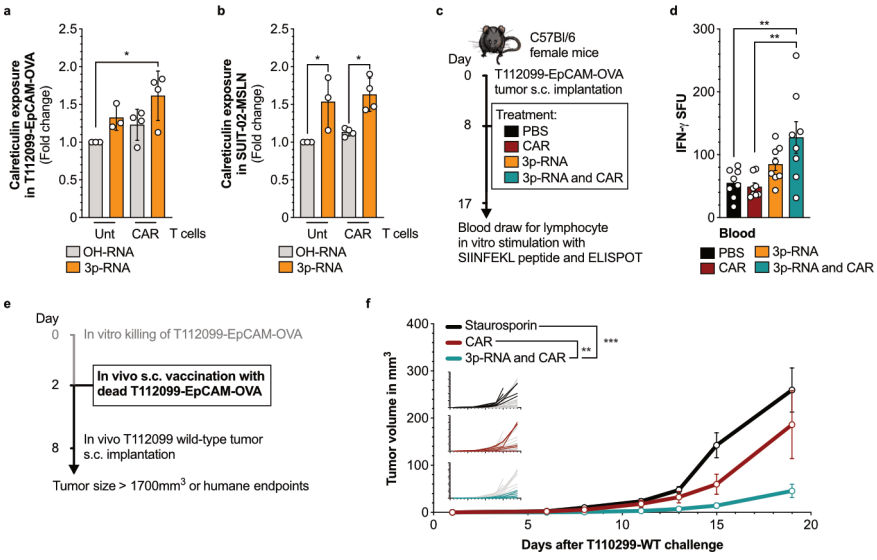

Figure 4 3p-RNA-induced ICD enhances antigen presentation and spreading. (a) Flow cytometry analysis of calreticulin exposure in in vitro assays using T110299-EpCAM-OVA, and (b) SUIT-2-MSLN tumor cells transfected with 3p-RNA for 24 hours, followed by in vitro co-culture with CAR-T cells for additional 24 hours. (c) Experimental layout where mice with T110299-EpCAM-OVA tumors were treated with 10 µg of in vivo-JetPEI-complexed 3p-RNA and/or 10^7 adoptively transferred T cells (at least 30% were anti-EpCAM CAR-T cells). Nine days post-treatment, leukocytes were isolated, stimulated with SIINFEKL peptide, and IFN-γ production quantified by ELISpot, data depicted in (d). (e) Experimental layout for tumor antigen spreading after vaccination with killed tumor cell debris. (f) T110299-EpCAM-OVA cells were killed in vitro with anti-EpCAM CAR-T cells alone, CAR-T cells together with 3p-RNA or Staurosporin, and cell debris was used to vaccinate naïve mice by s.c. injection in the right flank. 8 days later, mice were challenged with antigen-negative T110299 tumor cells s.c. injected in the left flank, and tumor volume was monitored. Error bars represent mean±SEM. Individual plots show the tumor growth of each mouse in a specific group, colored, vs. the tumor growth of each mouse in other groups, gray. Statistical analysis was performed using one-way ANOVA or two-way ANOVA with Tukey's multiple comparisons. *p<0.05, **p<0.01, ***p<0.001, **** p<0.0001. ANOVA, analysis of variance; ICD, immunogenic cell death; s.c., subcutaneous.

(figure 4c). 9 days post-treatment, IFN-γ ELISpot analysis of peripheral blood T cells revealed a significant increase in OVA-specific spot-forming units (SFU) in the 3p-RNA and CAR combination group compared with CAR-T cell monotherapy (figure 4d). Although 3p-RNA monotherapy induces a measurable OVA-specific ELISpot response consistent with its known ability to trigger ICD, only the combination therapy leads to tumor eradication and relapse protection. Thus, the ELISpot signal reflects initiation of antigen spreading but does not predict therapeutic potency. These findings were further supported by a vaccination assay—the gold standard for evaluating ICD (figure 4e,f). Tumor cells were pretreated for 48 hours with CAR-T cells alone, CAR-T cells together with 3p-RNA, or staurosporine as a non-ICD inducing control,[21] ensuring complete cell killing. Killed tumor cells were then injected subcutaneously into naïve mice (figure 4e). Upon subsequent challenge with CAR antigen-negative wild-type tumor cells 8 days later, mice vaccinated with 3p-RNA/CAR-T cell-killed cells exhibited improved tumor control compared with those vaccinated with cells killed by CAR-T cells or staurosporine alone (figure 4f). The vaccination study does not allow a 3p-RNA-only control group because 3p-RNA does not lead to sufficient cell death in vitro; therefore, we cannot quantify the 3p-RNA specific contributions. Nevertheless, in the therapeutic experiments, 3p-RNA monotherapy did not induce tumor eradication, whereas only the 3p-RNA and CAR-T combination produced durable control, increased CAR-T persistence, and TME remodeling. Collectively, these data indicate that CAR-T cells alone induce limited immunogenicity and antigen spreading. The addition of 3p-RNA markedly enhances ICD and promotes de novo neoantigen-specific T cell responses—an effect that may help prevent relapse driven by antigen loss.

DISCUSSION

This study demonstrates that preconditioning of the TME by intratumoral 3p-RNA treatment converts refractory PDAC into CAR-T cell responsive disease by overcoming key immunologic and microenvironmental barriers. Our findings show that RIG-I activation in murine and human PDAC tumor models enhances CAR-T cell activation, degranulation, and cytotoxicity, as evidenced by increased expression of CD69, IFN-γ, and Granzyme B, as well as faster tumor cell killing. While 3p-RNA-monotherapy does not lead to sufficient tumor clearance, it initiates antigen spreading through ICD, and the combination with CAR-T cells converts this initial signal into durable, polyclonal antitumor immunity. Thus, 3p-RNA serves as an initiator of immunogenicity, but CAR-T effector function is indispensable for therapeutic translation of antigen spreading. These findings are in line with recent studies highlighting the potential of RNA-based immunomodulatory approaches to enhance T cell-based therapies.[34 35]

Beyond direct enhancement of CAR-T cell cytotoxicity, 3p-RNA treatment profoundly reshaped the TME. In line with previous reports from our group, 3p-RNA treatment shifted the balance of myeloid cells from immunosuppressive TANs and TAMs to pro-inflammatory Ly-6C$^+$ monocytes.[11] Our treatment schedule for 3p-RNA was restricted to two injections due to the rapid but transient kinetics of RIG-I activation (higher dosages offer limited benefit while increasing local toxicity).[11 21] The increased immune cell infiltration in the xenograft model indicates that part of the 3p-RNA effect is mediated by conserved tumor-intrinsic RIG-I biology rather than strictly by host immunity. Overlapping the second dose of 3p-RNA with infiltration and expansion of adoptively transferred CAR-T cells enabled us to maximize RIG-I-driven chemokine induction and CAR-T recruitment in the tumor models probed. This combination drives epitope spreading and abscopal control, unlike either monotherapy, highlighting innate cues as amplifiers of durable T cell immunity.[36] RIG-I-driven type I IFN and ICD enhance MHC-I expression in DCs as shown in this study, most likely leading to antigen cross-presentation and CD8$^+$ T cell priming.[33] Importantly, this bystander recruitment effect should also be valid for endogenous T cells, suggesting that the combination strategy may synergize with endogenous immunity.[37] In vitro migration assays further showed that specifically the CCR5-expressing and CXCR3-expressing T cells preferentially migrated toward 3p-RNA-transfected tumor cells, implicating the importance of the CCL4-5/CCR5 and CXCL9-11/CXCR3 axes in the observed enhanced CAR-T recruitment. This is consistent with earlier work showing that immunogenic chemotherapy and CAR-T combinations generate an initial CCR5-dependent influx and a CXCR3-driven second wave of infiltration in response to IFN-γ-induced chemokines.[15] It is plausible that the enhanced infiltration we observed in our study may also be driven by these known orchestrators of tumor trafficking, CXCR3- and/or CCR5.[38]

Our study sheds light on the poorly understood relationship between CAR-T cell therapy and antigen spreading. While antigen spreading has been recognized as a hallmark of durable antitumor responses,[39 40] it remains an open question whether CAR-T cells alone can induce robust antigen spreading. Emerging evidence suggests that CAR-T cell-mediated cytotoxicity, in the absence of additional immunologic cues, is insufficient to elicit strong endogenous T cell responses against bystander tumor antigens. For instance, Ma *et al* showed that vaccine-boosted CAR-T cells, but not CAR-T monotherapy, elicited robust antigen spreading by promoting DC recruitment and activation via IFN-γ signaling.[41] Likewise, Guo *et al* emphasized the critical role of antigen-presenting cell activation in driving endogenous T cell priming following CAR-T cell treatment.[42] ICD plays a key role in activating DCs and promoting antigen uptake and cross-presentation, thereby driving de novo T cell responses against non-target tumor antigens.[33] Using an isolated cellular in vitro model and a vaccination approach, our data validate that CAR-T cells alone have limited capacity to induce ICD marker and antigen-spreading. Notably, the combination with 3p-RNA rescues the immunogenicity of the induced cell death, thereby offering a novel approach to mitigate antigen loss-mediated relapse in CAR-T cell therapy.

This study primarily relied on murine and xenograft models, and species- or model-specific contributions cannot be entirely excluded. Despite model-specific considerations—for example, different transfection efficacies across SUIT-2 and KPC-derived murine PDAC cell lines,[43–45] or higher RIG-I pathway expression and responsiveness in human PDAC cell lines including SUIT-2,[19 20] the translational relevance of RIG-I stimulation to human cancer therapy is well supported. The RIG-I/RLR-interferon axis is evolutionarily conserved and mediates a canonical type I IFN and chemokine response across species.[46] Moreover, the enhanced CAR-T infiltration we observed in our human SUIT-2 xenograft model, which lacks adaptive immunity, indicates that at least part of the 3p-RNA effect is mediated by tumor-intrinsic RIG-I activation, rather than exclusively by host immune circuitries. Importantly, synthetic RIG-I agonists, including IVT RNAs and stem-loop RNAs, have entered early-phase clinical trials (eg, NCT03739138, NCT04096638, NCT02828098), and have shown favorable safety profiles. Early clinical experience with PEI-complexed RLR-agonists supports the feasibility of intratumoral administration without severe toxicity (NCT03739138, NCT02828098). Local injection poses practical challenges, but emerging systemic delivery platforms, including ionizable lipid nanoparticles and targeted nanoparticles, have demonstrated the ability to deliver immunostimulatory RNAs to tumors and activate RIG-I/IFN pathways,[47 48] and early-phase clinical studies of systemically administered innate agonists (eg, SB-11285) are under way (NCT04096638). These developments underscore the feasibility of translating localized RIG-I activation into clinical settings and highlight its potential value in human PDAC, where immune exclusion and insufficient antigenicity remain dominant mechanisms of resistance.

Although our data reveal a clear role for 3p-RNA in restoring immunogenicity and enabling antigen spreading, several mechanistic questions remain. Quantifying antigen spreading with endogenous antigen assays, such as gp70 tetramers or an unbiased neo-epitope screen, would clarify the breadth of epitope diversification triggered by 3p-RNA-enhanced CAR-T therapy. These analyses lie beyond the scope of the current work, but they present a rational roadmap to strengthen translational confidence.

Our study establishes cytosolic RIG-I agonism with 3p-RNA as a fully synthetic lever to overcome immune exclusion in solid tumors. By triggering a tumor-focused type I interferon burst, 3p-RNA increases CAR-T cell infiltration, drives ICD, and broadens antigen recognition, culminating in durable tumor control in stringent PDAC models.

Author affiliations
[1]Institute of Clinical Pharmacology, LMU University Hospital, LMU Munich, Munich, Germany
[2]Department of Internal Medicine III, Hematology and Oncology, University Hospital Regensburg, Regensburg, Germany
[3]Department of Medicine II, LMU University Hospital, LMU Munich, Munich, Germany
[4]German Cancer Consortium (DKTK), a partnership between LMU Klinikum and DKFZ, Heidelberg, Germany
[5]Einheit für Klinische Pharmakologie (EKLiP), Helmholtz Zentrum Munchen Deutsches Forschungszentrum fur Gesundheit und Umwelt Gmbh, Neuherberg, Germany
[6]Institute of Innate Immunity, University Hospital Bonn, Bonn, Germany
[7]German Center for Lung Research (DZL), Munich, Germany

Acknowledgements Cytometry data were obtained in the Core Facility Flow Cytometry of the University Hospital, LMU Munich.

Contributors Conceptualization: AS and LK. Methodology: AS, BLC, JT, SF, CM, and TL. Formal analysis: AS, BLC, JT, and TL. Investigation: AS, BLC, JT, SF, CM, TL, DFRB, CH, SD, and LK. Resources: SE, MS, PD, SK, and LK. Writing–original draft: AS, BLC, PD, and LK. Writing–review and editing: AS, BLC, JT, TL, CM, CH, SE, MS, PD, SK, and LK. Visualization: AS, BLC, JT, PD, and LK. Supervision: LK. Project administration: SE, MS, PD, SK, and LK. Funding acquisition: SE, MS, PD, SK, and LK. Guarantor: LK.

Funding This work was supported by: the Deutsche Forschungsgemeinschaft (DFG, German Research Foundation) project 442265435 to LK; CRC–237/A28 to LK (project-ID 369799452); 329628492 SFB 1321 to MS; 432325352 SFB 1454 to PD; the Stiftungen zugunsten der Medizinischen Fakultät–Cluster 1 to LK; the Marie-Sklodowska-Curie Training Network for the Immunotherapy of Cancer (IMMUTRAIN, grant number 641549) funded by the H2020 program of the European Union to SE, MS and SK; the international doctoral program "iTarget: Immunotargeting of cancer" funded by the Elite Network of Bavaria to LK, MS, SK and SE; the Bavarian Cancer Research Center (BZKF) (TANGO to SK), the Else Kröner-Fresenius Stiftung (2023_EKEA.60) to CM, the Deutsche Forschungsgemeinschaft (DFG, grant number KO5055/3-1 to SK), Marie Sklodowska-Curie Training Network for tracking and controlling therapeutic immune cells in cancer (funded by the Horizon Programme of the EU, grant 101168810 to SK), Else KrönerKröner-Fresenius-Stiftung (IOLIN to SK), German Cancer Aid (DEFEAT PDAC and AvantCAR.de to SK), the Wilhelm-Sander-Stiftung (to SK), Ernst Jung Stiftung (to SK), Bundesministerium fürfür Bildung und Forschung (to SE and SK), the EUROSTAR-Programm (to SK), European Research Council (PoC Grant 101100460 and CoG 101124203 to SK), by the SFB-TRR 338/1 2021–452881907 (to SK), Fritz-Bender Foundation (to SK), Deutsche José Carreras Leukämie Stiftung (to SK), Bavarian Research Foundation (BAYCELLATOR to SK), the Monika-Kutzner Foundation (to SK), the Bruno and Helene Jöster Foundation (360° CAR to SK), the Brigitte and Dr. Konstanze Wegener (to SK), the Dr. RurainskiFoundation Rurainski Foundation (to SK).

Competing interests AS and LK are now employees of BioNTech without relation to this work. SK has received honoraria from Regeneron, Plectonic, TCR2, Miltenyi, Galapagos, Cymab, Novartis, BMS, and GSK. SK is an inventor of several patents in the field of immuno-oncology. SK and SE received license fees from TCR2 Inc and Carina Biotech. SK received research support from TCR2, Tabby Therapeutics, Catalym, Plectonic, and Arcus Bioscience for work unrelated to the manuscript. All other authors declare no competing interests.

Patient consent for publication Not applicable.

Provenance and peer review Not commissioned; externally peer reviewed.

Data availability statement All data relevant to the study are included in the article or uploaded as supplementary information. Further information and requests for resources and reagents should be directed to and will be fulfilled by the lead contact, LK (lars.koenig@med.uni-muenchen.de).

ORCID iDs
Stefan Endres https://orcid.org/0000-0002-4703-537X

Peter Duewell https://orcid.org/0000-0003-0836-6448
Sebastian Kobold https://orcid.org/0000-0002-5612-4673
Lars M Koenig https://orcid.org/0000-0002-8348-7787

REFERENCES

1 Siegel RL, Giaquinto AN, Jemal A. Cancer statistics, 2024. *CA Cancer J Clin* 2024;74:12–49.
2 Beatty GL, O'Hara MH, Lacey SF, *et al*. Activity of Mesothelin-Specific Chimeric Antigen Receptor T Cells Against Pancreatic Carcinoma Metastases in a Phase 1 Trial. *Gastroenterology* 2018;155:29–32.
3 Newick K, O'Brien S, Moon E, *et al*. CAR T Cell Therapy for Solid Tumors. *Annu Rev Med* 2017;68:139–52.
4 Qi C, Liu C, Gong J, *et al*. Claudin18.2-specific CAR T cells in gastrointestinal cancers: phase 1 trial final results. *Nat Med* 2024;30:2224–34.
5 Qi C, Liu C, Peng Z, *et al*. Claudin-18 isoform 2-specific CAR T-cell therapy (satri-cel) versus treatment of physician's choice for previously treated advanced gastric or gastro-oesophageal junction cancer (CT041-ST-01): a randomised, open-label, phase 2 trial. *The Lancet* 2025;405:2049–60.
6 Marabelle A, Fakih M, Lopez J, *et al*. Association of tumour mutational burden with outcomes in patients with advanced solid tumours treated with pembrolizumab: prospective biomarker analysis of the multicohort, open-label, phase 2 KEYNOTE-158 study. *Lancet Oncol* 2020;21:1353–65.
7 Stein MN, Dumbrava EE, Teply BA, *et al*. PSCA-targeted BPX-601 CAR T cells with pharmacological activation by rimiducid in metastatic pancreatic and prostate cancer: a phase 1 dose escalation trial. *Nat Commun* 2024;15:10743.
8 Özdemir BC, Pentcheva-Hoang T, Carstens JL, *et al*. Depletion of carcinoma-associated fibroblasts and fibrosis induces immunosuppression and accelerates pancreas cancer with reduced survival. *Cancer Cell* 2014;25:719–34.
9 Provenzano PP, Cuevas C, Chang AE, *et al*. Enzymatic targeting of the stroma ablates physical barriers to treatment of pancreatic ductal adenocarcinoma. *Cancer Cell* 2012;21:418–29.
10 Elyada E, Bolisetty M, Laise P, *et al*. Cross-Species Single-Cell Analysis of Pancreatic Ductal Adenocarcinoma Reveals Antigen-Presenting Cancer-Associated Fibroblasts. *Cancer Discov* 2019;9:1102–23.
11 Metzger P, Kirchleitner SV, Kluge M, *et al*. Immunostimulatory RNA leads to functional reprogramming of myeloid-derived suppressor cells in pancreatic cancer. *J Immunother Cancer* 2019;7:288.
12 Metzger P, Kirchleitner SV, Boehmer DFR, *et al*. Systemic but not MDSC-specific IRF4 deficiency promotes an immunosuppressed tumor microenvironment in a murine pancreatic cancer model. *Cancer Immunol Immunother* 2020;69:2101–12.
13 Majzner RG, Mackall CL. Tumor Antigen Escape from CAR T-cell Therapy. *Cancer Discov* 2018;8:1219–26.
14 Kluger H, Barrett JC, Gainor JF, *et al*. Society for Immunotherapy of Cancer (SITC) consensus definitions for resistance to combinations of immune checkpoint inhibitors. *J Immunother Cancer* 2023;11:e005921.
15 Srivastava S, Furlan SN, Jaeger-Ruckstuhl CA, *et al*. Immunogenic Chemotherapy Enhances Recruitment of CAR-T Cells to Lung Tumors and Improves Antitumor Efficacy when Combined with Checkpoint Blockade. *Cancer Cell* 2021;39:193–208.
16 Tran E, Turcotte S, Gros A, *et al*. Cancer Immunotherapy Based on Mutation-Specific CD4+ T Cells in a Patient with Epithelial Cancer. *Science* 2014;344:641–5.
17 Minute L, Teijeira A, Sanchez-Paulete AR, *et al*. Cellular cytotoxicity is a form of immunogenic cell death. *J Immunother Cancer* 2020;8:e000325.
18 Jaime-Sanchez P, Uranga-Murillo I, Aguilo N, *et al*. Cell death induced by cytotoxic $CD8^+$ T cells is immunogenic and primes caspase-3-dependent spread immunity against endogenous tumor antigens. *J Immunother Cancer* 2020;8:e000528.
19 Soliman N, Nedelko T, Mandracci G, *et al*. Targeting Intracellular Innate RNA-Sensing Systems Overcomes Resistance to CAR T-cell Therapy in Solid Tumors. *Cancer Res* 2025;85:2679–93.
20 Hornung V, Ellegast J, Kim S, *et al*. 5'-Triphosphate RNA Is the Ligand for RIG-I. *Science* 2006;314:994–7.
21 Duewell P, Steger A, Lohr H, *et al*. RIG-I-like helicases induce immunogenic cell death of pancreatic cancer cells and sensitize tumors toward killing by CD8(+) T cells. *Cell Death Differ* 2014;21:1825–37.
22 Karches CH, Benmebarek M-R, Schmidbauer ML, *et al*. Bispecific Antibodies Enable Synthetic Agonistic Receptor-Transduced T Cells for Tumor Immunotherapy. *Clin Cancer Res* 2019;25:5890–900.
23 Cadilha BL, Benmebarek M-R, Dorman K, *et al*. Combined tumor-directed recruitment and protection from immune suppression enable CAR T cell efficacy in solid tumors. *Sci Adv* 2021;7:eabi5781.
24 Kobold S, Grassmann S, Chaloupka M, *et al*. Impact of a New Fusion Receptor on PD-1-Mediated Immunosuppression in Adoptive T Cell Therapy. *J Natl Cancer Inst* 2015;107:djv146.
25 Rapp M, Grassmann S, Chaloupka M, *et al*. C-C chemokine receptor type-4 transduction of T cells enhances interaction with dendritic cells, tumor infiltration and therapeutic efficacy of adoptive T cell transfer. *Oncoimmunology* 2016;5:e1105428.
26 Lesch S, Blumenberg V, Stoiber S, *et al*. T cells armed with C-X-C chemokine receptor type 6 enhance adoptive cell therapy for pancreatic tumours. *Nat Biomed Eng* 2021;5:1246–60.
27 Uslu U, June CH. Beyond the blood: expanding CAR T cell therapy to solid tumors. *Nat Biotechnol* 2025;43:506–15.
28 Boehmer DFR, Formisano S, Oliveira Mann CC, *et al*. OAS1/RNase L executes RIG-I ligand–dependent tumor cell apoptosis. *Sci Immunol [Internet] American Association for the Advancement of Science* 2021. Available: https://doi.org/10.1126/SCIIMMUNOL.ABE2550/SUPPL_FILE/SCIIMMUNOL.ABE2550_SM.PDF
29 Larson RC, Maus MV. Recent advances and discoveries in the mechanisms and functions of CAR T cells. *Nat Rev Cancer* 2021;21:145–61.
30 Solstad A, Hogaboam O, Forero A, *et al*. RIG-I-like Receptor Regulation of Immune Cell Function and Therapeutic Implications. *J Immunol* 2022;209:845–54.
31 Pietrobon V, Todd LA, Goswami A, *et al*. Improving CAR T-Cell Persistence. *Int J Mol Sci* 2021;22:10828.
32 Mempel TR, Lill JK, Altenburger LM. How chemokines organize the tumour microenvironment. *Nat Rev Cancer* 2024;24:28–50.
33 Fucikova J, Kepp O, Kasikova L, *et al*. Detection of immunogenic cell death and its relevance for cancer therapy. *Cell Death Dis* 2020;11:1013.
34 Nissim L, Wu M-R, Pery E, *et al*. Synthetic RNA-Based Immunomodulatory Gene Circuits for Cancer Immunotherapy. *Cell* 2017;171:1138–50.
35 Jiang Y, Zhang Z, Wang W, *et al*. Biology-guided deep learning predicts prognosis and cancer immunotherapy response. *Nat Commun* 2023;14:5135.
36 Conde E, Vercher E, Soria-Castellano M, *et al*. Epitope spreading driven by the joint action of CART cells and pharmacological STING stimulation counteracts tumor escape via antigen-loss variants. *J Immunother Cancer* 2021;9:e003351. Available: https://doi.org/10.1136/jitc-2021-003351
37 Johnson LR, Lee DY, Eacret JS, *et al*. The immunostimulatory RNA RN7SL1 enables CAR-T cells to enhance autonomous and endogenous immune function. *Cell* 2021;184:4981–95.
38 Ozga AJ, Chow MT, Luster AD. Chemokines and the immune response to cancer. *Immunity* 2021;54:859–74.
39 Azulay M, Shahar M, Shany E, *et al*. Tumor-targeted superantigens produce curative tumor immunity with induction of memory and demonstrated antigen spreading. *J Transl Med* 2023;21:222.
40 Brossart P. The Role of Antigen Spreading in the Efficacy of Immunotherapies. *Clin Cancer Res* 2020;26:4442–7.
41 Ma L, Hostetler A, Morgan DM, *et al*. Vaccine-boosted CAR T crosstalk with host immunity to reject tumors with antigen heterogeneity. *Cell* 2023;186:3148–65.
42 Guo Y, Tong C, Wu Z, *et al*. Reciprocal activation of antigen-presenting cells and CAR T cells triggers a widespread endogenous anti-tumor immune response through sustained high-level IFNγ production. *Cancer Biol Med* 2023;20:779–82.
43 Chong ZX, Yeap SK, Ho WY. Transfection types, methods and strategies: a technical review. *PeerJ [Internet] PeerJ* 2021. Available: https://doi.org/10.7717/PEERJ.11165
44 Tonack S, Patel S, Jalali M, *et al*. Tetracycline-inducible protein expression in pancreatic cancer cells: Effects of CapG overexpression. *World J Gastroenterol* 2011;17:1947. Available: https://doi.org/10.3748/WJG.V17.I15.1947
45 Pirona AC, Oktriani R, Boettcher M, *et al*. Process for an efficient lentiviral cell transduction. *Biol Methods Protoc* 2020;5:bpaa005.
46 Rehwinkel J, Gack MU. RIG-I-like receptors: their regulation and roles in RNA sensing. *Nat Rev Immunol* 2020;20:537–51.
47 Wang-Bishop L, Wehbe M, Pastora LE, *et al*. Nanoparticle Retinoic Acid-Inducible Gene I Agonist for Cancer Immunotherapy. *ACS Nano* 2024;18:11631–43.
48 Yoshida S, Miyagawa S, Fukushima S, *et al*. Maturation of Human Induced Pluripotent Stem Cell-Derived Cardiomyocytes by Soluble Factors from Human Mesenchymal Stem Cells. *Mol Ther* 2018;26:2681–95.